Implicit Kernel Learning

Chun-Liang Li **Wei-Cheng Chang** **Youssef Mroueh** **Yiming Yang** **Barnabás Póczos**
{chunlial, wchang2, yiming, bapoczos}@cs.cmu.edu mroueh@us.ibm.com
Carnegie Mellon University and IBM Research

Abstract

Kernels are powerful and versatile tools in machine learning and statistics. Although the notion of *universal kernels* and *characteristic kernels* has been studied, kernel selection still greatly influences the empirical performance. While learning the kernel in a data driven way has been investigated, in this paper we explore learning the spectral distribution of kernel via implicit generative models parametrized by deep neural networks. We called our method *Implicit Kernel Learning* (IKL). The proposed framework is simple to train and inference is performed via sampling random Fourier features. We investigate two applications of the proposed IKL as examples, including generative adversarial networks with MMD (MMD GAN) and standard supervised learning. Empirically, MMD GAN with IKL outperforms vanilla predefined kernels on both image and text generation benchmarks; using IKL with Random Kitchen Sinks also leads to substantial improvement over existing state-of-the-art kernel learning algorithms on popular supervised learning benchmarks. Theory and conditions for using IKL in both applications are also studied as well as connections to previous state-of-the-art methods.

1 Introduction

Kernel methods are among the essential foundations in machine learning and have been extensively studied in the past decades. In supervised learning, kernel methods allow us to learn non-linear hypothesis. They also play a crucial role in statistics. Kernel maximum mean discrepancy (MMD) (Gretton et al., 2012) is a powerful two-sample test, which is based on a statistics computed via kernel functions. Even though there is a surge of deep learning in the past years, several successes have been shown by kernel methods and deep feature extraction. Wilson et al. (2016) demonstrate state-of-the-art performance by incorporating deep learning, kernel and Gaussian process. Li et al. (2015); Dziugaite et al. (2015) use MMD to train deep generative models for complex datasets.

In practice, however, kernel selection is always an important step. Instead of choosing by a heuristic, several works have studied *kernel learning*. Multiple kernel learning (MKL) (Bach et al., 2004; Lanckriet et al., 2004; Bach, 2009; Gönen and Alpaydın, 2011; Duvenaud et al., 2013) is one of the pioneering frameworks to combine predefined kernels. One recent kernel learning development is to learn kernels via learning spectral distributions (Fourier transform of the kernel). Wilson and Adams (2013) model spectral distributions via a mixture of Gaussians, which can also be treated as an extension of linear combination of kernels (Bach et al., 2004). Oliva et al. (2016) extend it to Bayesian nonparametric models. In addition to model spectral distribution with *explicit* density models aforementioned, many works optimize the sampled random features or its weights (e.g. Băzăvan et al. (2012); Yang et al. (2015); Sinha and Duchi (2016); Chang et al. (2017); Bullins et al. (2018)). The other orthogonal approach to modeling spectral distributions is learning feature maps for standard kernels (e.g. Gaussian). Feature maps learned by deep learning lead to state-of-the-art performance on different tasks (Hinton and Salakhutdinov, 2008; Wilson et al., 2016; Li et al., 2017).

In addition to learning effective features, implicit generative models via deep learning also lead to promising performance in learning distributions of complex data (Goodfellow et al., 2014). Inspired by its recent success, we propose to model kernel spectral distributions with implicit generative models in a data-driven fashion, which we call *Implicit Kernel Learning* (IKL). IKL provides a new route to modeling spectral distri-

Proceedings of the 22nd International Conference on Artificial Intelligence and Statistics (AISTATS) 2019, Naha, Okinawa, Japan. PMLR: Volume 89.

butions by learning sampling processes of the spectral densities, which is under explored by previous works aforementioned.

In this paper, we start from studying the generic problem formulation of IKL, and propose an easily implemented, trained and evaluated neural network parameterization which satisfies Bochner's theorem (Section 2). We then demonstrate two example applications of the proposed IKL. Firstly, we explore MMD GAN (Li et al., 2017) with IKL on learning to generate images and text (Section 3). Secondly, we consider a standard two-staged supervised learning task with Random Kitchen Sinks (Sinha and Duchi, 2016) (Section 4). The conditions required for training IKL and its theoretical guarantees in both tasks are also studied. In both tasks, we show that IKL leads to competitive or better performance than heuristic kernel selections and existing approaches modeling kernel spectral densities. It demonstrates the potentials of learning more powerful kernels via deep generative models. Finally, we discuss the connection with existing works in Section 5.

2 Kernel Learning

Kernels have been used in several applications with success, including supervised learning, unsupervised learning, and hypothesis testing. They have also been combined with deep learning in different applications (Mairal et al., 2014; Li et al., 2015; Dziugaite et al., 2015; Wilson et al., 2016; Mairal, 2016). Given data $x \in \mathbb{R}^d$, kernel methods compute the inner product of the feature transformation $\phi(x)$ in a high-dimensional Hilbert space H via a kernel function $k : \mathcal{X} \times \mathcal{X} \to \mathbb{R}$, which is defined as $k(x, x') = \langle \phi(x), \phi(x') \rangle_H$, where $\phi(x)$ is usually high or even infinitely dimensional. If k is shift invariant (i.e. $k(x, y) = k(x - y)$), we can represent k as an expectation with respect to a spectral distribution $\mathbb{P}_k(\omega)$.

Bochner's theorem (Rudin, 2011) A continuous, real valued, symmetric and shift-invariant function k on $\mathbb{R}^d$ is a positive definite kernel if and only if there is a positive finite measure $\mathbb{P}_k(\omega)$ such that

$$k(x-x') = \int_{\mathbb{R}^d} e^{i\omega^\top (x-x')} d\mathbb{P}_k(\omega) = \mathbb{E}_{\omega \sim \mathbb{P}_k} \left[e^{i\omega^\top (x-x')} \right].$$

2.1 Implicit Kernel Learning

We restrict ourselves to learning shift invariant kernels. According to that, learning kernels is equivalent to learning a spectral distribution by optimizing

$$\begin{aligned} &\arg\max_{k \in \mathcal{K}} \sum_{i=1} \mathbb{E}_{x \sim \mathbb{P}_i, x' \sim \mathbb{Q}_i} \left[F_i(x, x') k(x, x') \right] = \\ &\arg\max_{k \in \mathcal{K}} \sum_{i=1} \mathbb{E}_{x \sim \mathbb{P}_i, x' \sim \mathbb{Q}_i} \left[F_i(x, x') \mathbb{E}_{\omega \sim \mathbb{P}_k} \left[e^{i\omega^\top (x-x')} \right] \right], \end{aligned} \tag{1}$$

where F is a task-specific objective function and $\mathcal{K}$ is a set of kernels. (1) covers many popular objectives, such as kernel alignment (Gönen and Alpaydın, 2011) and MMD distance (Gretton et al., 2012). Existing works (Wilson and Adams, 2013; Oliva et al., 2016) learn the spectral density $\mathbb{P}_k(\omega)$ with *explicit* forms via parametric or non-parametric models. When we learn kernels via (1), it may not be necessary to model the density of $\mathbb{P}_k(\omega)$, as long as we are able to estimate kernel evaluations $k(x - x') = \mathbb{E}_\omega[e^{i\omega^\top (x-x')}]$ via sampling from $\mathbb{P}_k(\omega)$ (Rahimi and Recht, 2007). Alternatively, *implicit probabilistic (generative) models* define a stochastic procedure that can generate (sample) data from $\mathbb{P}_k(\omega)$ without modeling $\mathbb{P}_k(\omega)$. Recently, the neural implicit generative models (MacKay, 1995) regained attentions with promising results (Goodfellow et al., 2014) and simple sampling procedures. We first sample ν from a base distribution $\mathbb{P}(\nu)$ which is known (e.g. Gaussian distribution), then use a deterministic function h_ψ parametrized by ψ, to transform ν into $\omega = h_\psi(\nu)$, where ω follows the complex target distribution $\mathbb{P}_k(\omega)$. Inspired by the success of deep implicit generative models (Goodfellow et al., 2014), we propose an *Implicit Kernel Learning (IKL)* method by modeling $\mathbb{P}_k(\omega)$ via an implicit generative model $h_\psi(\nu)$, where $\nu \sim \mathbb{P}(\nu)$, which results in

$$k_\psi(x, x') = \mathbb{E}_\nu \left[e^{i h_\psi(\nu)^\top (x-x')} \right] \tag{2}$$

and reducing (1) to solve

$$\arg\max_{\psi} \sum_{i=1} \mathbb{E}_{x \sim \mathbb{P}_i, x' \sim \mathbb{Q}_i} \left[F_i(x, x') \mathbb{E}_\nu \left(e^{i h_\psi(\nu)^\top (x-x')} \right) \right]. \tag{3}$$

The gradient of (3) can be represented as

$$\sum_{i=1} \mathbb{E}_{x \sim \mathbb{P}_i, x' \sim \mathbb{Q}_i} \mathbb{E}_\nu \left[\nabla_\psi F_i(x, x') e^{i h_\psi(\nu)^\top (x-x')} \right].$$

Thus, (3) can be optimized via sampling x, x' from data and ν from the base distribution to estimate gradient as shown above (SGD) in every iteration. Next, we discuss the parametrization of h_ψ to satisfy Bochner's Theorem, and describe how to evaluate IKL kernel in practice.

Symmetric $\mathbb{P}_k(\omega)$ To result in real valued kernels, the spectral density has to be symmetric, where $\mathbb{P}_k(\omega) = \mathbb{P}_k(-\omega)$. Thus, we parametrize $h_\psi(\nu) =$

$\texttt{sign}(\nu) \circ \tilde{h}_\psi(\texttt{abs}(\nu))$, where $\circ$ is the Hadamard product and $\tilde{h}_\psi$ can be any unconstrained function if the base distribution $\mathbb{P}(\nu)$ is symmetric (i.e. $\mathbb{P}(\nu) = \mathbb{P}(-\nu)$), such as standard normal distributions.

Kernel Evaluation Although there is usually no closed form for the kernel evaluation $k_\psi(x, x')$ in (2) with fairly complicated h_ψ, we can evaluate (approximate) $k_\psi(x, x')$ via sampling finite number of random Fourier features $\hat{k}_\psi(x, x') = \hat{\phi}_{h_\psi}(x)^\top \hat{\phi}_{h_\psi}(x')$, where $\hat{\phi}_{h_\psi}(x)^\top = [\phi(x; h_\psi(\nu_1)), \dots, \phi(x; h_\psi(\nu_m))]$, and $\phi(x; \omega)$ is the evaluation on ω of the Fourier transformation $\phi(x)$ (Rahimi and Recht, 2007).

Next, we demonstrate two example applications covered by (3), where we can apply IKL, including kernel alignment and maximum mean discrepancy (MMD).

3 MMD GAN with IKL

Given $\{x_i\}_{i=1}^n \sim \mathbb{P}_\mathcal{X}$, instead of estimating the density $\mathbb{P}_\mathcal{X}$, Generative Adversarial Network (GAN) (Goodfellow et al., 2014) is an implicit generative model, which learns a generative network g_θ (generator). The generator g_θ transforms a base distribution $\mathbb{P}_\mathcal{Z}$ over $\mathcal{Z}$ into $\mathbb{P}_\theta$ to approximate $\mathbb{P}_\mathcal{X}$, where $\mathbb{P}_\theta$ is the distribution of $g_\theta(z)$ and $z \sim \mathbb{P}_\mathcal{Z}$. During the training, GAN alternatively estimates a *distance* $D(\mathbb{P}_\mathcal{X} \| \mathbb{P}_\theta)$ between $\mathbb{P}_\mathcal{X}$ and $\mathbb{P}_\theta$, and updates g_θ to minimize $D(\mathbb{P}_\mathcal{X} \| \mathbb{P}_\theta)$. Different probability metrics have been studied (Goodfellow et al., 2014; Li et al., 2015; Dziugaite et al., 2015; Nowozin et al., 2016; Arjovsky et al., 2017; Mroueh et al., 2017; Li et al., 2017; Mroueh and Sercu, 2017; Gulrajani et al., 2017; Mroueh et al., 2018; Arbel et al., 2018) for training GANs.

Kernel maximum mean discrepancy (MMD) is a probability metric, which is commonly used in two-sample-test to distinguish two distributions with finite samples (Gretton et al., 2012). Given a kernel k, the MMD between $\mathbb{P}$ and $\mathbb{Q}$ is defined as

$$M_k(\mathbb{P}, \mathbb{Q}) = \mathbb{E}_{\mathbb{P},\mathbb{P}}[k(x, x')] - 2\mathbb{E}_{\mathbb{P},\mathbb{Q}}[k(x, y)] + \mathbb{E}_{\mathbb{Q},\mathbb{Q}}[k(y, y')]. \tag{4}$$

For characteristic kernels, $M_k(\mathbb{P}, \mathbb{Q}) = 0$ *iff* $\mathbb{P} = \mathbb{Q}$. Li et al. (2015); Dziugaite et al. (2015) train the generator g_θ by optimizing $\min_\theta M_k(\mathbb{P}_\mathcal{X}, \mathbb{P}_\theta)$ with a Gaussian kernel k. Li et al. (2017) propose MMD GAN, which trains g_θ via $\min_\theta \max_{k \in \mathcal{K}} M_k(\mathbb{P}_\mathcal{X}, \mathbb{P}_\theta)$, where $\mathcal{K}$ is a pre-defined set of kernels. The intuition is to learn a kernel $\operatorname{argmax}_{k \in \mathcal{K}} M_k(\mathbb{P}_\mathcal{X}, \mathbb{P}_\theta)$, which has a stronger signal (i.e. larger distance when $\mathbb{P}_\mathcal{X} \neq \mathbb{P}_\theta$) to train g_θ. Specifically, Li et al. (2017) consider a composition kernel k_φ which combines Gaussian kernel k and a neural network f_φ as $k_\varphi = k \circ f_\varphi$, where

$$k_\varphi(x, x') = \exp(-\|f_\varphi(x) - f_\varphi(x')\|^2). \tag{5}$$

The MMD GAN objective then becomes $\min_\theta \max_\varphi M_\varphi(\mathbb{P}_\mathcal{X}, \mathbb{P}_\theta)$.

3.1 Training MMD GAN with IKL

Although the composition kernel with a learned feature embedding f_φ is powerful, choosing a good base kernel k is still crucial in practice (Bińkowski et al., 2018). Different base kernels for MMD GAN, such as rational quadratic kernel (Bińkowski et al., 2018) and distance kernel (Bellemare et al., 2017), have been studied. Instead of choosing it by hands, we propose to learn the base kernel by IKL, which extend (5) to be $k_{\psi,\varphi} = k_\psi \circ f_\varphi$ with the form

$$k_{\psi,\varphi}(x, x') = \mathbb{E}_\nu \left[e^{i h_\psi(\nu)^\top (f_\varphi(x) - f_\varphi(x'))} \right]. \tag{6}$$

We then extend the MMD GAN objective to be

$$\min_\theta \max_{\psi,\varphi} M_{\psi,\varphi}(\mathbb{P}_\mathcal{X}, \mathbb{P}_\theta), \tag{7}$$

where $M_{\psi,\varphi}$ is the MMD distance (4) with the IKL kernel (6). Clearly, for a given φ, the maximization over ψ in (7) can be represented as (1) by letting $F_1(x, x') = 1$, $F_2(x, y) = -2$ and $F_3(y, y') = 1$. In what follows, we will use for convenience $k_{\psi,\varphi}$, k_ψ and k_φ to denote kernels defined in (6), (2) and (5) respectively.

3.2 Property of MMD GAN with IKL

As proven by Arjovsky and Bottou (2017), some probability distances adopted by existing works (e.g. Goodfellow et al. (2014)) are not *weak* (i.e. $\mathbb{P}_n \xrightarrow{D} \mathbb{P}$ then $D(\mathbb{P}_n \| \mathbb{P}) \to 0$), which cannot provide better signal to train g_θ. Also, they usually suffer from discontinuity, hence it cannot be trained via gradient descent at certain points. We prove that $\max_{\psi,\varphi} M_{\psi,\varphi}(\mathbb{P}_\mathcal{X}, \mathbb{P}_\theta)$ is a continuous and differentiable objective in θ and *weak* under mild assumptions as used in (Arjovsky et al., 2017; Li et al., 2017).

Assumption 1. *$g_\theta(z)$ is locally Lipschitz and differentiable in θ; $f_\varphi(x)$ is Lipschitz in x and $\varphi \in \Phi$ is compact. $f_\varphi \circ g_\theta(z)$ is differentiable in θ and there are local Lipschitz constants, which is independent of φ, such that $\mathbb{E}_{z \sim \mathbb{P}_z}[L(\theta, z)] < +\infty$. The above assumptions are adopted by Arjovsky et al. (2017). Lastly, assume given any $\psi \in \Psi$, where Ψ is compact, $k_\psi(x, x') = \mathbb{E}_\nu \left[e^{i h_\psi(\nu)^\top (x - x')} \right]$ and $|k_\psi(x, x')| < \infty$ is differentiable and Lipschitz in (x, x') which has an upper bound L_k for Lipschitz constant of (x, x') given different ψ.*

Theorem 2. *Assume function g_θ and kernel $k_{\psi,\varphi}$ satisfy Assumption 1, $\max_{\psi,\varphi} M_{\psi,\varphi}$ is weak, that is, $\max_{\psi,\varphi} M_{\psi,\varphi}(\mathbb{P}_\mathcal{X}, \mathbb{P}_n) \to 0 \iff \mathbb{P}_n \xrightarrow{D} \mathbb{P}_\mathcal{X}$. Also,*

$\max_{\psi,\varphi} M_{\psi,\varphi}(\mathbb{P}_\mathcal{X}, \mathbb{P}_\theta)$ *is continuous everywhere and differentiable almost everywhere in* θ.

Lemma 3. *Assume* $\mathcal{X}$ *is bounded. Let* $x, x' \in \mathcal{X}$, $k_\psi(x, x') = \mathbb{E}_\nu\left[e^{ih_\psi(\nu)^\top(x-x')}\right]$ *is Lipschitz in* (x, x') *if* $\mathbb{E}_\nu\left[\|h_\psi(\nu)\|^2\right] < \infty$, *which is variance since* $\mathbb{E}_\nu\left[h_\psi(\nu)\right] = 0$.

We penalize $\lambda_h(\mathbb{E}_\nu\left[\|h_\psi(\nu)\|^2\right] - u)^2$ as an approximation of Lemma 3 in practice to ensure that assumptions in Theorem 2 are satisfied. The algorithm with IKL and gradient penalty (Bińkowski et al., 2018) is shown in Algorithm 1.

Algorithm 1: MMD GAN with IKL

Input: η the learning rate, B the batch size, n_c number of f, h updates per g update, m the number of basis, λ_{GP} the coefficient of gradient penalty, λ_h the coefficient of variance constraint.
Initial parameter θ for g, φ for f, ψ for h
Define $\mathcal{L}(\psi, \varphi) = M_{\psi,\varphi}(\mathbb{P}_\mathcal{X}, \mathbb{P}_\theta) - \lambda_{GP}(\|\nabla_{\hat{x}} f_\varphi(\hat{x})\|_2 - 1)^2 - \lambda_h(\mathbb{E}_\nu[\|h_\psi(\nu)\|^2] - u)^2$
while θ has not converged **do**
  for $t = 1, \ldots, n_c$ **do**
    Sample $\{x_i\}_{i=1}^B \sim \mathbb{P}(\mathcal{X})$, $\{z_j\}_{j=1}^B \sim \mathbb{P}(\mathcal{Z})$, $\{\nu_k\}_{k=1}^m \sim \mathbb{P}(\nu)$
    $(\psi, \varphi) \leftarrow \varphi + \eta\text{Adam}\left((\psi, \varphi), \nabla_{\psi,\varphi}\mathcal{L}(\psi, \varphi)\right)$
  end for
  Sample $\{x_i\}_{i=1}^B \sim \mathbb{P}(\mathcal{X})$, $\{z_j\}_{j=1}^B \sim \mathbb{P}(\mathcal{Z})$, $\{\nu_k\}_{k=1}^m \sim \mathbb{P}(\nu)$
  $\theta \leftarrow \theta - \eta\text{Adam}(\theta, \nabla_\theta M_{\psi,\varphi}(\mathbb{P}_\mathcal{X}, \mathbb{P}_\theta))$
end while

3.3 Empirical Study

We consider image and text generation tasks for quantitative evaluation. For image generation, we evaluate the inception score (Salimans et al., 2016) and FID score (Heusel et al., 2017) on CIFAR-10 (Krizhevsky and Hinton, 2009). We use DCGAN (Radford et al., 2016) and expands the output of f_φ to be 16-dimensional as Bińkowski et al. (2018). For text generation, we consider a length-32 character-level generation task on Google Billion Words dataset. The evaluation is based on Jensen-Shannon divergence on empirical 4-gram probabilities (JS-4) of the generated sequence and the validation data as used by Gulrajani et al. (2017); Heusel et al. (2017); Mroueh et al. (2018). The model architecture follows Gulrajani et al. (2017) in using ResNet with 1D convolutions. We train every algorithm 10,000 iterations for comparison.

For MMD GAN with fixed base kernels, we consider the mixture of Gaussian kernels $k(x, x') = \sum_q \exp(-\frac{\|x-x'\|^2}{2\sigma_q^2})$ (Li et al., 2017) and the mixture of RQ kernels $k(x, x') = \sum_q (1 + \frac{\|x-x'\|^2}{2\alpha_q})^{-\alpha_q}$. We tuned hyperparameters σ_q and α_q for each kernel as reported in Appendix F.1.

Lastly, for learning base kernels, we compare IKL with SM kernel (Wilson and Adams, 2013) f_φ, which learns mixture of Gaussians to model kernel spectral density. It can also be treated as the *explicit generative model counter part* of the proposed IKL.

In both tasks, $\mathbb{P}(\nu)$, the base distribution of IKL, is a standard normal distribution and h_ψ is a 3-layer MLP with 32 hidden units for each layer. Similar to the aforementioned mixture kernels, we consider the mixture of IKL kernel with the variance constraints $\mathbb{E}[\|h_\psi(\nu)\|^2] = 1/\sigma_q$, where σ_q is the bandwidths for the mixture of Gaussian kernels. Note that if h_ψ is an identity map, we recover the mixture of Gaussian kernels. We fix λ_h to be 10 and resample $m = 1024$ random features for IKL in every iteration. For other settings, we follow Bińkowski et al. (2018) and the hyperparameters can be found in Appendix F.1.

3.3.1 Results and Discussion

We compare MMD GAN with the proposed IKL and different fixed kernels. We repeat the experiments 10 times and report the average result with standard error in Table 1. Note that for inception score the larger the better; while JS-4 the smaller the better. We also report WGAN-GP results as a reference. Since FID score results (Heusel et al., 2017) is consistent with inception score and does not change our discussion, we put it in Appendix C.1 due to space limit. Sampled images on larger datasets are shown in Figure 1.

Method	Inception Scores (↑)	JS-4 (↓)
Gaussian	6.726 ± 0.021	0.381 ± 0.003
RQ	6.785 ± 0.031	0.463 ± 0.005
SM	6.746 ± 0.031	0.378 ± 0.003
IKL	$\mathbf{6.876 \pm 0.018}$	$\mathbf{0.372 \pm 0.002}$
WGAN-GP	6.539 ± 0.034	0.379 ± 0.002

Table 1: Inception scores and JS-4 divergece results.

Pre-defined Kernels Bińkowski et al. (2018) show RQ kernels outperform Gaussian and energy distance kernels on image generation. Our empirical results agree with such finding: RQ kernels achieve 6.785 inception score while for Gaussian kernel it is 6.726, as shown in the left column of Table 1. In text generation, nonetheless, RQ kernels only achieve 0.463 JS-4 score[1] and are not on par with 0.381 acquired by Gaus-

[1]For RQ kernels, we searched 10 possible hyperparameter settings and reported the best one in Appendix, to ensure the unsatisfactory performance is not caused by the improper parameters.

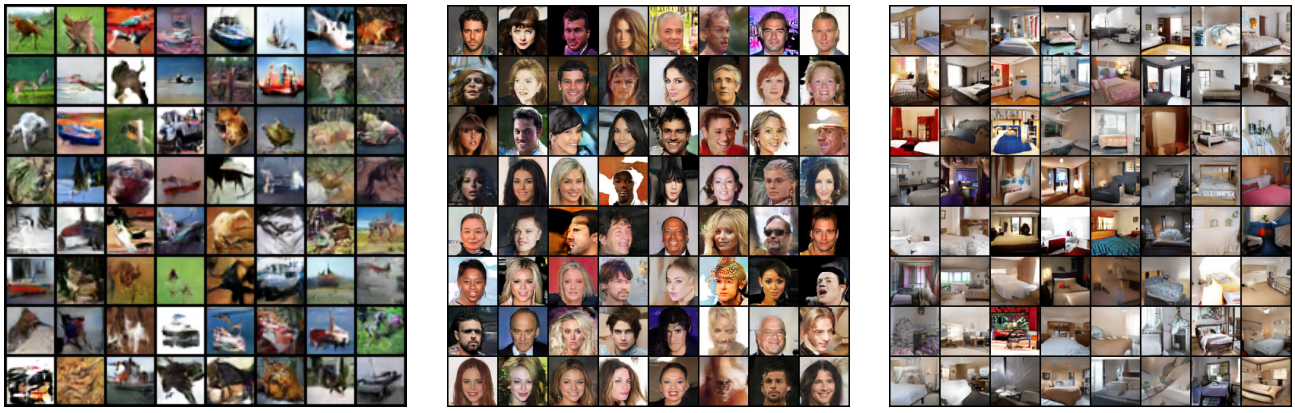

Figure 1: Samples generated by MMDGAN-IKL on CIFAR-10, CELEBA and LSUN dataset.

sian kernels, even though it is still slightly worse than WGAN-GP. These results imply *kernel selection is task-specific*. On the other hand, the proposed IKL learns kernels in a data-driven way, which results in the best performance in both tasks. In CIFAR-10, although Gaussian kernel is worse than RQ, IKL is still able to transforms $\mathbb{P}(\nu)$, which is Gaussian, into a powerful kernel, and outperforms RQ on inception scores (6.876 v.s. 6.785). For text generation, from Table 1 and Figure 2, we observe that IKL can further boost Gaussian into better kernels with substantial improvement. Also, we note that the difference between IKL and pre-defined kernels in Table 1 is significant based on the t-test at 95% confidence level.

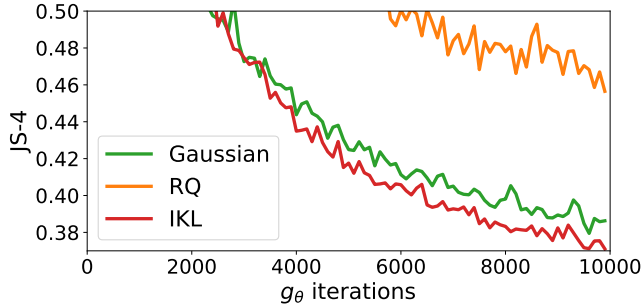

Figure 2: Convergence of MMD GANs with different kernels on text generation.

Learned Kernels The SM kernel (Wilson and Adams, 2013), which learns the spectral density via mixture of Gaussians, does not significantly outperforms Gaussian kernel as shown in Table 1, since Li et al. (2017) already uses equal-weighted mixture of Gaussian formulation. It suggests that proposed IKL can learn more complicated and effective spectral distributions than simple mixture models.

Study of Variance Constraints In Lemma 3, we prove bounding variance $\mathbb{E}[\|h_\psi(\nu)\|^2]$ guarantees k_ψ to be Lipschitz as required in Theorem 2. We investigate the importance of this constraint. In Figure 3, we show the training objective (MMD), $\mathbb{E}[\|h_\psi(\nu)\|^2]$ and the JS-4 divergence for training MMD GAN (IKL) without variance constraint, i.e. $\lambda_h = 0$. We could observe the variance keeps going up without constraints, which leads exploded MMD values. Also, when the exploration is getting severe, the JS-4 divergence starts increasing, which implies MMD cannot provide meaningful signal to g_θ. The study justifies the validity of Theorem 2 and Lemma 3.

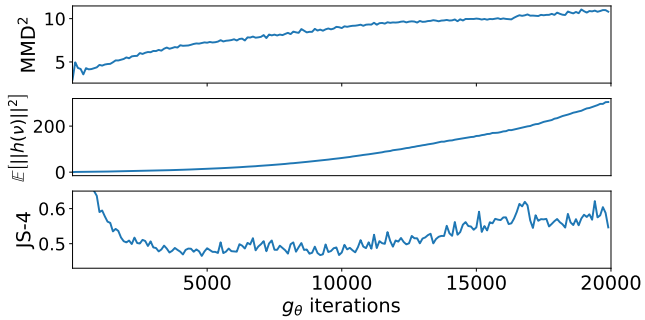

Figure 3: Learning MMD GAN (IKL) without the variance constraint on Google Billion Words datasets for text generation.

Other Studies One concern of the proposed IKL is the computational overhead introduced by sampling random features as well as using more parameters to model h_ψ. Since we only use small network to model h_ψ, the increased computation overhead is almost negligible under GPU parallel computation. The detailed comparison can be found in Appendix C.2. We also compare IKL with Bullins et al. (2018), which can be seen as a variant of IKL without h_ψ, and studt the variance constraint. Those additional discussions can be found in Appendix C.1.

4 Random Kitchen Sinks with IKL

Rahimi and Recht (2009) propose *Random Kitchen Sinks* (RKS) as follows. We sample $\omega_i \sim \mathbb{P}_k(\omega)$ and

transform $x \in \mathbb{R}^d$ into $\hat{\phi}(x) = [\phi(x;\omega_1), \ldots, \phi(x;\omega_M)]$, where $\sup_{x,\omega} |\phi(x;\omega)| < 1$. We then learn a classifier on the transformed features $\hat{\phi}(x;\omega)$. Kernel methods with random features (Rahimi and Recht, 2007) is an example of RKS, where $\mathbb{P}_k(\omega)$ is the spectral distribution of the kernel and $\phi(x;\omega) = \left[\cos(\omega^\top x), \sin(\omega^\top x)\right]$. We usually learn a model $\mathbf{w}$ by solving

$$\arg\min_{\mathbf{w}} \frac{\lambda}{2}\|\mathbf{w}\|^2 + \frac{1}{n}\sum_{i=1}^{n} \ell\left(\mathbf{w}^\top \hat{\phi}(x_i)\right). \tag{8}$$

If ℓ is a convex loss function, the objective (8) can be solved efficiently to global optimum.

Spectral distributions $\mathbb{P}_k$ are usually set as a parameterized form, such as Gaussian distributions, but the selection of $\mathbb{P}_k$ is important in practice. If we consider RKS as kernel methods with random features, then selecting $\mathbb{P}$ is equivalent to the well-known kernel selection (learning) problem for supervised learning (Gönen and Alpaydın, 2011).

Two-Stage Approach We follows Sinha and Duchi (2016) to consider kernel learning for RKS with a two-stage approach. In stage 1, we consider kernel alignment (Cristianini et al., 2002) of the form, $\operatorname{argmax}_{k\in\mathcal{K}} \mathbb{E}_{(x,y),(x',y')} \sum_{i\neq j} yy' k(x,x')$. By parameterizing k via the implicit generative model h_ψ as in Section 2, we have the following problem:

$$\operatorname*{argmax}_{\psi} \mathbb{E}_{(x,y),(x',y')} yy' \mathbb{E}_{\nu}\left[e^{ih_\psi(\nu)^\top (x-x')},\right]. \tag{9}$$

which can be treated as (1) with $F_1(x,x') = yy'$. After solving (9), we learn a *sampler* h_ψ where we can easily sample. Thus, in stage 2, we thus have the advantage of solving a convex problem (8) in RKS with IKL. The algorithm is shown in Algorithm 2.

Note that in stage 1, we resample $\{\nu_j\}_{j=1}^m$ in every iteration to train an implicit generative model h_ψ. The advantage of Algorithm 2 is the random features used in kernel learning and RKS can be *different*, which allows us to use *less* random features in kernel learning (stage 1), and sample *more* features for RKS (stage 2).

One can also *jointly* train both feature mapping ω and the model parameters $\mathbf{w}$, such as neural networks. We remark that our intent is not to show state-of-the-art results on supervised learning, on which deep neural networks dominate (Krizhevsky et al., 2012; He et al., 2016). We use RKS as a protocol to study kernel learning and the proposed IKL, which still has competitive performance with neural networks on some tasks (Rahimi and Recht, 2009; Sinha and Duchi, 2016). Also, the simple procedure of RKL with IKL allows us to provide some theoretical guarantees of the performance, which is sill challenging of deep learning models.

Algorithm 2: Random Kitchen Sinks with IKL

Stage 1: Kernel Learning

Input: $X = \{(x_i, y_i)\}_{i=1}^n$, the batch size B for data and m for random feature, learning rate η

Initial parameter ψ for h

while ψ has not converged or reach maximum iters **do**

Sample $\{(x_i, y_i)\}_{i=1}^B \subseteq X$. Fresh sample $\{\nu_j\}_{j=1}^m \sim \mathbb{P}(\nu)$

$g_\psi \leftarrow$ $\nabla_\psi \frac{1}{B(B-1)} \sum_{i\neq i'} y_i y_{i'} \frac{1}{m} \sum_{j=1}^m e^{ih_\psi(\nu_j)^\top (x_i - x_{i'})}$

$\psi \leftarrow \psi - \eta \mathrm{Adam}(\psi, g_\psi)$

end while

Stage 2: Random Kitchen Sinks

Sample $\{\nu_i\}_{i=1}^M \sim \mathbb{P}(\nu)$, note that M is not necessarily equal to m

Transform X into $\phi(X)$ via h_ψ and $\{\nu_i\}_{i=1}^M$

Learn a linear classifier on $(\phi(X), Y)$

Comparison with Existing Works Sinha and Duchi (2016) learn non-uniform weights for M random features via kernel alignment in stage 1 then using these optimized features in RKS in the stage 2. Note that the random features used in stage 1 has to be the same as the ones in stage 2. A jointly training of feature mapping and classifier can be treated as a 2-layer neural networks (Băzăvan et al., 2012; Alber et al., 2017; Bullins et al., 2018). Learning kernels with aforementioned works will be more costly if we want to use a large number of random features for training classifiers. In contrast to implicit generative models, Oliva et al. (2016) learn an explicit Bayesian nonparametric generative model for spectral distributions, which requires specifically designed inference algorithms. Learning kernels for (8) in dual form without random features has also been proposed. It usually require costly steps, such as eigendecomposition of the Gram matrix (Gönen and Alpaydın, 2011).

4.1 Empirical Study

We evaluate the proposed IKL on both synthetic and benchmark binary classification tasks. For IKL, $\mathbb{P}(\nu)$ is standard Normal and h_ψ is a 3-layer MLP for all experiments. The number of random features m to train h_ψ in Algorithm 2 is fixed to be 64. Other experiment details are described in Appendix F.2.

Kernel learning with a poor choice of $\mathbb{P}_k(\omega)$ We generate $\{x_i\}_{i=1}^n \sim \mathcal{N}(0, I_d)$ with $y_i = \mathrm{sign}(\|x\|_2 - \sqrt{d})$, where d is the data dimension. A two dimensional example is shown in Figure 4. Competitive baselines include random features (RFF) (Rahimi and Recht, 2007) as well as OPT-KL (Sinha and Duchi, 2016).

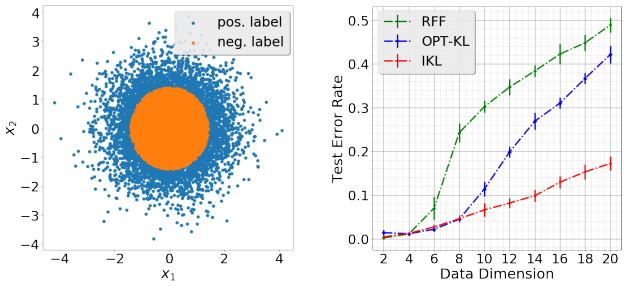

Figure 4: Left figure is training examples when $d = 2$. Right figure is the classification error v.s. data dimension.

In the experiments, we fix $M = 256$ in RKS for all algorithms. Since Gaussian kernels with the bandwidth $\sigma = 1$ is known to be ill-suited for this task (Sinha and Duchi, 2016), we directly use random features from it for RFF and OPT-KL. Similarly, we set $\mathbb{P}(\nu)$ to be standard normal distribution as well.

The test error for different data dimension $d = \{2, 4, \ldots, 18, 20\}$ is shown in Figure 4. Note that RFF is competitive with OPT-KL and IKL when d is small ($d \leq 6$), while its performance degrades rapidly as d increases, which is consistent with the observation in Sinha and Duchi (2016). More discussion of the reason of failure can be referred to Sinha and Duchi (2016). On the other hand, although using standard normal as the spectral distribution is ill-suited for this task, both OPT-KL and IKL can adapt with data and learn to transform it into effective kernels and result in slower degradation with d.

Note that OPT-KL learns the *sparse* weights on the sampled random features ($M = 256$). However, the sampled random features can fail to contain informative ones, especially in high dimension (Bullins et al., 2018). Thus, when using limited amount of random features, OPT-IKL may result in worse performance than IKL in the high dimensional regime in Figure 4.

Performance on benchmark datasets Next, we evaluate our IKL framework on standard benchmark binary classification tasks. Challenging label pairs are chosen from MNIST (LeCun et al., 1998) and CIFAR-10 (Krizhevsky and Hinton, 2009) datasets; each task consists of 10000 training and 2000 test examples. For all datasets, raw pixels are used as the feature representation. We set the bandwidth of RBF kernel by the median heuristic. We also compare with Wilson and Adams (2013), the spectral mixture (SM) kernel, which uses Gaussian mixture to learn spectral density and can be seen as the explicit generative model counterpart of IKL. Also, SM kernel is a MKL variant with linear combination (Gönen and Alpaydın, 2011). In addition, we consider the joint training of random features and model parameters, which can be treated as two-layer neural network (NN) and serve as the lower bound of error for comparing different kernel learning algorithms.

The test error versus different $M = \{2^6, 2^7, \ldots, 2^{13}\}$ in the second stage are shown in Figure 5. First, in light of computation efficiency, SM and the proposed IKL only sample $m = 64$ random features in each iteration in the first stage, and draws different number of basis M from the learned $h_\psi(\nu)$ for the second stage. OPT-KL, on the contrary, the random features used in training and testing should be the same. Therefore, OPT-IKL needs to deal with M random features in the training. It brings computation concern when M is large. In addition, IKL demonstrates improvement over the representative kernel learning method OPT-KL, especially significant on the challenging datasets such as CIFAR-10. In some cases, IKL almost reaches the performance of NN, such as MNIST, while OPT-KL degrades to RFF except for small number of basis ($M = 2^6$). This illustrates the effectiveness of learning kernel spectral distribution via the implicit generative model h_ψ. Also, IKL outperforms SM, which is consistent with the finding in Section 3 that IKL can learn more complicated spectral distributions than simple mixture models (SM).

4.2 Consistency and Generalization

The simple two-stages approach, IKL with RKS, allows us to provide the consistency and generalization guarantees. For consistency, it guarantees the solution of finite sample approximations of (9) approach to the optimum of (9) (population optimum), when we increase number of training data and number of random features. We firstly define necessary symbols and state the theorem.

Let $s(x_i, x_j) = y_i y_j$ be a label similarity function, where $|y_i| \leq 1$. We use s_{ij} to denote $s(x_i, x_j)$ interchangeably. Given a kernel k, we define the true and empirical alignment functions as,

$$\begin{aligned} T(k) &= \mathbb{E}\left[s(x, x')k(x, x')\right] \\ \hat{T}(k) &= \frac{1}{n(n-1)} \sum_{i \neq j} s_{ij} k(x_i, x_j). \end{aligned}$$

In the following, we abuse the notation k_ψ to be k_h for ease of illustration. Recall the definitions of $k_h(x, x') = \langle \phi_h(x), \phi_h(x') \rangle$ and $\hat{k}_h(x, x') = \hat{\phi}_h(x)^\top \hat{\phi}_h(x')$. We define two hypothesis sets

$$\begin{aligned} \mathcal{F}_\mathcal{H} &= \{f(x) = \langle w, \phi_h(x) \rangle_H | h \in \mathcal{H}, \langle w, w \rangle \leq 1\} \\ \hat{\mathcal{F}}^m_\mathcal{H} &= \{f(x) = w^\top \hat{\phi}_h(x) | h \in \mathcal{H}, \|w\| \leq 1, w \in \mathbb{R}^m\}. \end{aligned}$$

Definition 4. *(Rademacher's Complexity) Given a hypothesis set $\mathcal{F}$, where $f : \mathcal{X} \times \mathcal{X} \to \mathbb{R}$ if $f \in \mathcal{F}$,*

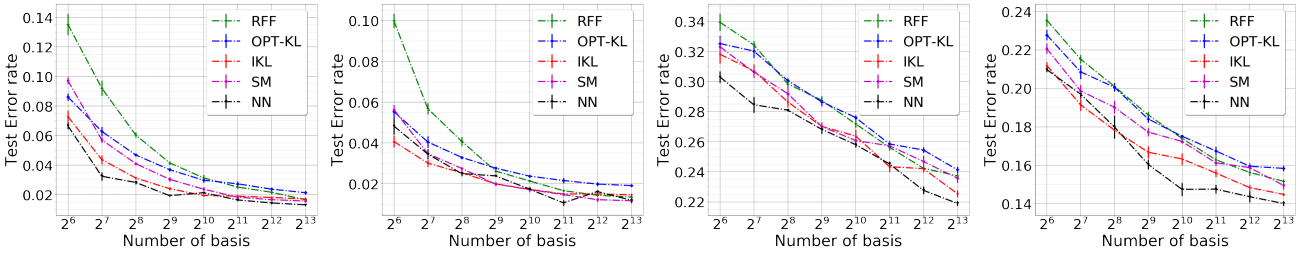

(a) MNIST (4-9) (b) MNIST (5-6) (c) CIFAR-10 (auto-truck) (d) CIFAR-10 (plane-bird)

Figure 5: Test error rate versus number of basis in second stage on benchmark binary classification tasks. We report mean and standard deviation over five runs. Our method (IKL) is compared with RFF (Rahimi and Recht, 2009), OPT-KL (Sinha and Duchi, 2016), SM (Wilson and Adams, 2013) and the end-to-end training MLP (NN).

and a fixed sample $X = \{x_1, \ldots, x_n\}$*, the empirical Rademacher's complexity of* $\mathcal{F}$ *is defined as*

$$\mathfrak{R}_X^n(\mathcal{F}) = \frac{1}{n}\mathbb{E}_\sigma\left[\sup_{f\in\mathcal{F}}\sum_{i=1}^n \sigma_i f(x_i)\right],$$

where σ *are* n *i.i.d. Rademacher random variables.*

We then have the following theorems showing that the consistency guarantee depends on the complexity of the function class induced by IKL as well as the number of random features. The proof can be found in Appendix D.

Theorem 5. *(Consistency) Let* $\hat{h} = \arg\max_{h\in\mathcal{H}} \hat{T}(\hat{k}_h)$*, with i.i.d, samples* $\{\nu_i\}_{i=1}^m$ *drawn from* $\mathbb{P}(\nu)$*. With probability at least* $1-3\delta$*, we have* $|T(\hat{k}_{\hat{h}}) - \sup_{h\in\mathcal{H}} T(k_h)| \leq$

$$2\mathbb{E}_X\left[\mathfrak{R}_X^{n-1}(\mathcal{F}_\mathcal{H}) + \mathfrak{R}_X^{n-1}(\hat{\mathcal{F}}_\mathcal{H}^m)\right] + \sqrt{\frac{8\log\frac{1}{\delta}}{n}} + \sqrt{\frac{2\log\frac{4}{\delta}}{m}}.$$

Applying Cortes et al. (2010), We also have a generalization bound, which depends number of training data n, number of random features m and the Rademacher complexity of IKL kernel, as shown in Appendix E. The Rademacher complexity $\mathfrak{R}_X^n(\mathcal{F}_\mathcal{H})$, for example, can be $1/\sqrt{n}$ or even $1/n$ for kernels with different bounding conditions (Cortes et al., 2013). We would expect worse rates for more powerful kernels. It suggests the trade-off between consistency/generalization and using powerful kernels parametrized by neural networks.

5 Discussion

We propose a generic kernel learning algorithm, IKL, which learns sampling processes of kernel spectral distributions by transforming samples from a base distribution $\mathbb{P}(\nu)$ into ones for the other kernel (spectral density). We compare IKL with other algorithms for learning MMD GAN and supervised learning with Random Kitchen Sinks (RKS). For these two tasks, the conditions and guarantees of IKL for are studied. Empirical studies show IKL is better than or competitive with the state-of-the-art kernel learning algorithms. It proves IKL can learn to transform $\mathbb{P}(\nu)$ into effective kernels even if $\mathbb{P}(\nu)$ is less less favorable to the task.

We note that the preliminary idea of IKL is mentioned in Băzăvan et al. (2012), but they ended up with a algorithm that directly optimizes sampled random features (RF), which has many follow-up works (e.g. Sinha and Duchi (2016); Bullins et al. (2018)). The major difference is, by learning the transformation function h_ψ, the RF used in training and evaluation can be different. This flexibility allows a simple training algorithm (SGD) and does not require to keep learned features. In our studies on GAN and RKS, we show using a simple MLP can already achieve better or competitive performance with those works, which suggest IKL can be a new direction for kernel learning and worth more studies.

We highlight that IKL is not conflict with existing works but can be combined with them. In Section 3, we show combining IKL with kernel learning via embedding (Wilson et al., 2016) and mixture of spectral distributions (Wilson and Adams, 2013). Therefore, in addition to the examples shown in Section 3 and Section 4, IKL is directly applicable to many existing works with kernel learning via embedding (e.g. Dai et al. (2014); Li and Póczos (2016); Wilson et al. (2016); Al-Shedivat et al. (2016); Arbel et al. (2018); Jean et al. (2018); Chang et al. (2019)). A possible extension is combining with Bayesian inference (Oliva et al., 2016) under the framework similar to Saatchi and Wilson (2017). The learned sampler from IKL can possibly provide an easier way to do Bayesian inference via sampling.

References

Al-Shedivat, M., Wilson, A. G., Saatchi, Y., Hu, Z., and Xing, E. P. (2016). Learning scalable deep kernels with recurrent structure. *arXiv preprint arXiv:1610.08936*.

Alber, M., Kindermans, P.-J., Schütt, K., Müller, K.-R., and Sha, F. (2017). An empirical study on the properties of random bases for kernel methods. In *NIPS*.

Arbel, M., Sutherland, D. J., Bińkowski, M., and Gretton, A. (2018). On gradient regularizers for mmd gans. In *NIPS*.

Arjovsky, M. and Bottou, L. (2017). Towards principled methods for training generative adversarial networks. In *ICLR*.

Arjovsky, M., Chintala, S., and Bottou, L. (2017). Wasserstein GAN. In *ICML*.

Bach, F. R. (2009). Exploring large feature spaces with hierarchical multiple kernel learning. In *NIPS*.

Bach, F. R., Lanckriet, G. R., and Jordan, M. I. (2004). Multiple kernel learning, conic duality, and the smo algorithm. In *ICML*.

Băzăvan, E. G., Li, F., and Sminchisescu, C. (2012). Fourier kernel learning. In *ECCV*.

Bellemare, M. G., Danihelka, I., Dabney, W., Mohamed, S., Lakshminarayanan, B., Hoyer, S., and Munos, R. (2017). The cramer distance as a solution to biased wasserstein gradients. *arXiv preprint arXiv:1705.10743*.

Bińkowski, M., Sutherland, D. J., Arbel, M., and Gretton, A. (2018). Demystifying mmd gans. In *ICLR*.

Borisenko, O. and Minchenko, L. (1992). Directional derivatives of the maximum function. *Cybernetics and Systems Analysis*, 28(2):309–312.

Bullins, B., Zhang, C., and Zhang, Y. (2018). Not-so-random features. In *ICLR*.

Chang, W.-C., Li, C.-L., Yang, Y., and Poczos, B. (2017). Data-driven random fourier features using stein effect. In *IJCAI*.

Chang, W.-C., Li, C.-L., Yang, Y., and Póczos, B. (2019). Kernel change-point detection with auxiliary deep generative models. *arXiv preprint arXiv:1901.06077*.

Cortes, C., Kloft, M., and Mohri, M. (2013). Learning kernels using local rademacher complexity. In *NIPS*.

Cortes, C., Mohri, M., and Rostamizadeh, A. (2010). Generalization bounds for learning kernels. In *ICML*.

Cristianini, N., Shawe-Taylor, J., Elisseeff, A., and Kandola, J. S. (2002). On kernel-target alignment. In *ICML*.

Dai, B., Xie, B., He, N., Liang, Y., Raj, A., Balcan, M.-F. F., and Song, L. (2014). Scalable kernel methods via doubly stochastic gradients. In *NIPS*.

Dudley, R. M. (2018). *Real Analysis and Probability*. Chapman and Hall/CRC.

Duvenaud, D., Lloyd, J. R., Grosse, R., Tenenbaum, J. B., and Ghahramani, Z. (2013). Structure discovery in nonparametric regression through compositional kernel search. In *ICML*.

Dziugaite, G. K., Roy, D. M., and Ghahramani, Z. (2015). Training generative neural networks via maximum mean discrepancy optimization. In *UAI*.

Fan, R.-E., Chang, K.-W., Hsieh, C.-J., Wang, X.-R., and Lin, C.-J. (2008). Liblinear: A library for large linear classification. *JMLR*.

Gönen, M. and Alpaydın, E. (2011). Multiple kernel learning algorithms. *JMLR*.

Goodfellow, I. J., Pouget-Abadie, J., Mirza, M., Xu, B., Warde-Farley, D., Ozair, S., Courville, A. C., and Bengio, Y. (2014). Generative adversarial nets. In *NIPS*.

Gretton, A., Borgwardt, K. M., Rasch, M. J., Schölkopf, B., and Smola, A. (2012). A kernel two-sample test. *JMLR*.

Gulrajani, I., Ahmed, F., Arjovsky, M., Dumoulin, V., and Courville, A. (2017). Improved training of wasserstein gans. In *NIPS*.

He, K., Zhang, X., Ren, S., and Sun, J. (2016). Deep residual learning for image recognition. In *CVPR*.

Heusel, M., Ramsauer, H., Unterthiner, T., Nessler, B., and Hochreiter, S. (2017). Gans trained by a two time-scale update rule converge to a local nash equilibrium. In *NIPS*.

Hinton, G. E. and Salakhutdinov, R. R. (2008). Using deep belief nets to learn covariance kernels for gaussian processes. In *NIPS*.

Jean, N., Xie, S. M., and Ermon, S. (2018). Semi-supervised deep kernel learning: Regression with unlabeled data by minimizing predictive variance. In *Advances in Neural Information Processing Systems*, pages 5327–5338.

Krizhevsky, A. and Hinton, G. (2009). Learning multiple layers of features from tiny images.

Krizhevsky, A., Sutskever, I., and Hinton, G. E. (2012). Imagenet classification with deep convolutional neural networks. In *NIPS*.

Lanckriet, G. R., Cristianini, N., Bartlett, P., Ghaoui, L. E., and Jordan, M. I. (2004). Learning the kernel matrix with semidefinite programming. *JMLR*.

LeCun, Y., Bottou, L., Bengio, Y., and Haffner, P. (1998). Gradient-based learning applied to document recognition. *Proceedings of the IEEE*.

Li, C.-L., Chang, W.-C., Cheng, Y., Yang, Y., and Poczos, B. (2017). Mmd gan: Towards deeper understanding of moment matching network. In *NIPS*.

Li, C.-L. and Póczos, B. (2016). Utilize old coordinates: Faster doubly stochastic gradients for kernel methods. In *UAI*.

Li, Y., Swersky, K., and Zemel, R. (2015). Generative moment matching networks. In *ICML*.

MacKay, D. J. (1995). Bayesian neural networks and density networks. *Nuclear Instruments and Methods in Physics Research Section A: Accelerators, Spectrometers, Detectors and Associated Equipment*.

Mairal, J. (2016). End-to-end kernel learning with supervised convolutional kernel networks. In *NIPS*.

Mairal, J., Koniusz, P., Harchaoui, Z., and Schmid, C. (2014). Convolutional kernel networks. In *NIPS*.

Mroueh, Y., Li, C.-L., Sercu, T., Raj, A., and Cheng, Y. (2018). Sobolev gan. In *ICLR*.

Mroueh, Y. and Sercu, T. (2017). Fisher gan. In *NIPS*.

Mroueh, Y., Sercu, T., and Goel, V. (2017). Mcgan: Mean and covariance feature matching gan. In *ICML*.

Nowozin, S., Cseke, B., and Tomioka, R. (2016). f-gan: Training generative neural samplers using variational divergence minimization. In *NIPS*.

Oliva, J. B., Dubey, A., Wilson, A. G., Póczos, B., Schneider, J., and Xing, E. P. (2016). Bayesian nonparametric kernel-learning. In *AISTATS*.

Radford, A., Metz, L., and Chintala, S. (2016). Unsupervised representation learning with deep convolutional generative adversarial networks. In *ICLR*.

Rahimi, A. and Recht, B. (2007). Random features for large-scale kernel machines. In *NIPS*.

Rahimi, A. and Recht, B. (2009). Weighted sums of random kitchen sinks: Replacing minimization with randomization in learning. In *NIPS*.

Rudin, W. (2011). *Fourier analysis on groups*. John Wiley & Sons.

Saatchi, Y. and Wilson, A. G. (2017). Bayesian gan. In *NIPS*, pages 3625–3634.

Salimans, T., Goodfellow, I., Zaremba, W., Cheung, V., Radford, A., and Chen, X. (2016). Improved techniques for training gans. In *NIPS*.

Sinha, A. and Duchi, J. C. (2016). Learning kernels with random features. In *NIPS*.

Wilson, A. and Adams, R. (2013). Gaussian process kernels for pattern discovery and extrapolation. In *ICML*.

Wilson, A. G., Hu, Z., Salakhutdinov, R., and Xing, E. P. (2016). Deep kernel learning. In *AISTATS*.

Yang, Z., Wilson, A., Smola, A., and Song, L. (2015). A la carte–learning fast kernels. In *AISTATS*.

Zhang, Y., Liang, P., and Charikar, M. (2017). A hitting time analysis of stochastic gradient langevin dynamics. In *COLT*.

A Proof of Theorem 2

We first show $\mathbb{P}_n \xrightarrow{D} \mathbb{P}$ then $\max_{\psi,\varphi} M_{\psi,\varphi}(\mathbb{P}, \mathbb{P}_n) \to 0$. The results are based on Arbel et al. (2018), which leverages Corollary 11.3.4 of Dudley (2018). Follows the sketch of Arbel et al. (2018), the only thing we remain to show is proving $\|k_\psi(f_\varphi(x), \cdot) - k_\psi(f_\varphi(y), \cdot)\|_{\mathcal{H}_K}$ is Lipschitz. By definition, we know that $\|k_\psi(f_\varphi(x), \cdot) - k_\psi(f_\varphi(y), \cdot)\|_{\mathcal{H}_K} = 2(1 - k_\psi(f_\varphi(x), f_\varphi(y)))$. Also, since $k_\psi(0) = 1$ and $k_\psi(0) - k_\psi(x, x') \leq L_k \|0 - (x - x')\|$ (Lipschtiz assumption of k_ψ), we have

$$\|k_\psi(f_\varphi(x), \cdot) - k_\psi(f_\varphi(y), \cdot)\|_{\mathcal{H}_K} \leq 2L_k \|f_\varphi(x) - f_\varphi(y)\| \leq 2L_k L \|x - y\|,$$

where the last inequality is since f_φ is also a Lipschitz function with Lipschitz constant L.

The other direction, $\max_{\psi,\varphi} M_{\psi,\varphi}(\mathbb{P}, \mathbb{P}_n) \to 0$ then $\mathbb{P}_n \xrightarrow{D} \mathbb{P}$, is relatively simple. Without loss of generality, we assume there exists ψ' and ϕ' such that h_ψ and f_ϕ are identity functions (up to scaling), which recover the Gaussian kernel k. Therefore, $\max_{\psi,\varphi} M_{\psi,\varphi}(\mathbb{P}, \mathbb{P}_n) \to 0$ implies $M_{\psi',\varphi'}(\mathbb{P}, \mathbb{P}_n) \to 0$, which completes the proof because MMD with any Gaussian kernel is weak (Gretton et al., 2012).

A.1 Continuity

Lemma 6. *(Borisenko and Minchenko (1992)) Define $\tau(x) = \max\{f(x, u) | u \in U\}$. If f is locally Lipschitz in x, U is compact and $\bigtriangledown f(x, u^*(x))$ exists, where $u^*(x) = \arg\max_u f(x, u)$, then $\tau(x)$ is differentiable almost everywhere.*

We are going to show

$$\max_{\psi,\varphi} M_{\psi,\varphi}(\mathbb{P}_\mathcal{X}, \mathbb{P}_\theta) = \mathbb{E}_{x,x'}[k_{\psi,\varphi}(x, x')] - 2\mathbb{E}_{x,z}[k_{\psi,\varphi}(x, g_\theta(z))] + \mathbb{E}_{z,z'}[k_{\psi,\varphi}(g_\theta(z'), g_\theta(z))] \tag{10}$$

is differentiable with respect to φ almost everywhere by using the auxiliary Lemma 6. We fist show $\mathbb{E}_{z,z'}[k_{\psi,\varphi}(g_\theta(z'), g_\theta(z))]$ in (10) is locally Lipschitz in θ. By definition, $k_{\psi,\varphi}(x, x') = k_\psi(f_\varphi(x) - f_\varphi(x'))$, therefore,

$$\begin{aligned}
&\mathbb{E}_{x,x'}\left[k_{\psi,\varphi}\Big(g_\theta(z), g_\theta(z')\Big) - k_{\psi,\varphi}\Big(g_{\theta'}(z), g_{\theta'}(z')\Big)\right] \\
=&\mathbb{E}_{z,z'}\left[k_\psi\Big(f_\varphi\big(g_\theta(z)\big) - f_\varphi\big(g_\theta(z')\big)\Big)\right] - \mathbb{E}_{z,z'}\left[k_\psi\Big(f_\varphi\big(g_{\theta'}(z)\big) - f_\varphi\big(g_{\theta'}(z')\big)\Big)\right] \\
\leq&\mathbb{E}_{z,z'}\left[L_k\Big\|f_\varphi\big(g_\theta(z)\big) - f_\varphi\big(g_\theta(z')\big) - f_\varphi\big(g_{\theta'}(z)\big) + f_\varphi\big(g_{\theta'}(z')\big)\Big\|\right] \\
\leq&\mathbb{E}_{z,z'}\Big[L_k L(\theta, z)\|\theta - \theta'\| + L_k L(\theta, z')\|\theta - \theta'\|\Big] \\
=&2L_k \mathbb{E}_z\big[L(\theta, z)\big]\|\theta - \theta'\|.
\end{aligned}$$

The first inequality is followed by the assumption that k is locally Lipschitz in (x, x'), with a upper bound L_k for Lipschitz constants. By Assumption 1, $\mathbb{E}_z\big[L(\theta, z)\big] < \infty$, we prove $\mathbb{E}_{z,z'}\Big[k_\psi\big(f_\varphi(g_\theta(z)) - f_\varphi(g_\theta(z'))\big)\Big]$ is locally Lipschitz. The similar argument is applicable to other terms in (10); therefore, (10) is locally Lipschitz in θ.

Last, with the compactness assumption on Φ and Ψ, and differentiable assumption on $M_{\psi,\varphi}(\mathbb{P}_\mathcal{X}, \mathbb{P}_\theta)$, applying Lemma 6 proves Theorem 2.

B Proof of Lemma 3

Without loss of the generality, we can rewrite the kernel function as $k_\psi(t) = \mathbb{E}_\nu\Big[\cos\big(h_\psi(\nu)^\top t\big)\Big]$, where t is bounded. We then have

$$\begin{aligned}
\|\nabla_t k_\psi(t)\| &= \Big\|\mathbb{E}_\nu\Big[\sin\big(h_\psi(\nu)^\top t\big)h_\psi(\nu)\Big]\Big\| \\
&\leq \mathbb{E}_\nu\Big[\big|\sin(h_\psi(\nu)^\top t)\big| \times \|h_\psi(\nu)\|\Big] \\
&\leq \mathbb{E}_\nu\big[\|t\|\|h_\psi(\nu)\|^2\big]
\end{aligned}$$

The last inequality follows by $|\sin(x)| < |x|$. Since t is bounded, if $\mathbb{E}_\nu[\|h_\psi(\nu)\|^2] < \infty$, there exist a constant L such that $\|\nabla_t k_\psi(t)\| < L, \forall t$.

By mean value theorem, for any t and t', there exists $s = \alpha t + (1-\alpha)t'$, where $\alpha \in [0,1]$, such that

$$k_\psi(t) - k_\psi(t') = \nabla_s k_\psi(s)^\top (t - t').$$

Combining with $\|\nabla_t k_\psi(t)\| < L, \forall t$, we prove

$$k_\psi(t) - k_\psi(t') \le L\|t - t'\|.$$

C Additional Studies of MMD GAN with IKL

C.1 Additional Quantitative Results

We show the full quantitative results on MMD GANs with different kernels with mean and standard error in Table 2. In every tasks, IKL is the best among the predefined base kernels (Gaussian, RQ) and the competitive kernel learning algorithm (SM). The difference in FID is less significant than inception score and JS-4, but we note that FID score is a biased evaluation metric as discussed in Bińkowski et al. (2018).

Method	Inception Scores (↑)	FID Scores (↓)	JS-4 (↓)
Gaussian	6.726 ± 0.021	32.50 ± 0.07	0.381 ± 0.003
RQ	6.785 ± 0.031	32.20 ± 0.09	0.463 ± 0.005
SM	6.746 ± 0.031	32.43 ± 0.08	0.378 ± 0.003
IKL	$\mathbf{6.876 \pm 0.018}$	$\mathbf{31.98 \pm 0.05}$	$\mathbf{0.372 \pm 0.002}$
WGAN-GP	6.539 ± 0.034	36.413 ± 0.05	0.379 ± 0.002

Table 2: Inception scores, FID scores, and JS-4 divergece results.

C.2 Computational Issues of GAN trainings with IKL

Model Capacity For f_φ, the number of parameters for DCGAN is around 0.8 million for size 32×32 images and 3 millions for size 64×64 images. The ResNet architecture used in Gulrajani et al. (2017) has around 10 millions parameters. In contrast, in all experiments, we use simple three layer MLP as h_ψ for IKL, where the input and output dimensions are 16, and hidden layer size is 32. The total parameters are just around 2,000. Compared with f_ϕ, the additional number of parameters used for h_ψ is almost negligible.

Computational Time The potential concern of IKL is sampling random features for each examples. In our experiments, we use $m = 1024$ random features for each iteration. We measure the time per iteration of updating critic iterations (f for WGAN-GP and MMD GAN with Gaussian kernel; f and h for IKL) with different batch sizes under Titan X. The difference between WGAN-GP, MMD GAN and IKL are not significant. The reason is computing MMD and random feature is highly parallelizable, and other computation, such as evaluating f_ϕ and its gradient penalty, dominates the cost because f_ϕ has much more parameters as aforementioned. Therefore, we believe the proposed IKL is still cost effective in practice.

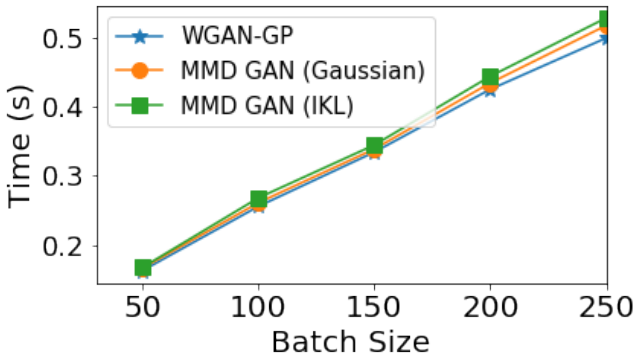

C.3 Detailed Discussion of Variance Constraints

In Section 3, we propose to constrain variance via $\lambda_h(\mathbb{E}_\nu\left[\|h_\psi(\nu)\|^2\right] - u)^2$. There are other alternatives, such as constraining L^2 penalty or using Langrange. In practice, we do not observe significant difference.

Although we show the necessity of the variance constraint in language generation in Figure 3, we remark that the proposed constraint is a sufficient condition. For CIFAR-10, without the constraint, we observe that the variance is still bouncing between 1 and 2 without explosion as Figure 3. Therefore, the training leads to a satisfactory result with 6.731 ± 0.034 inception score, but it is slightly worse than IKL in Table 1. The necessary or weaker sufficient conditions are worth further studying as a future work.

C.4 IKL with and without Neural Networks on GAN training

Instead of learning a transform function h_ψ for the spectral distribution as we proposed in Section 2 (IKL-NN), the other realization of IKL is to keep a pool of finite number learned random features $\Omega = \{\hat{\omega}_i\}_{i=1}^m$, and approximate the kernel evaluation by $\hat{k}_\Omega(x, x') = \hat{\phi}_\Omega(x)^\top \hat{\phi}_\Omega(x')$, where $\hat{\phi}_\Omega(x)^\top = [\phi(x; \hat{\omega}_1), \ldots, \phi(x; \hat{\omega}_m)]$. During the learning, it directly optimize $\hat{\omega}_i$. Many existing works study this idea for supervised learning, such as Băzăvan et al. (2012); Yang et al. (2015); Sinha and Duchi (2016); Chang et al. (2017); Bullins et al. (2018). We call the latter realization as IKL-RFF. Next, we discuss and compare the difference between IKL-NN and IKL-RFF.

The crucial difference between IKL-NN and IKL-RFF is, IKL-NN can sample arbitrary number of random features by first sampling $\nu \sim \mathbb{P}(\nu)$ and transforming it via $h_\psi(\nu)$, while IKL-RFF is restricted by the pool size m. If the application needs more random features, IKL-RFF will be memory inefficient. Specifically, we compare IKL-NN and IKL-RFF with different number of random features in Figure 6. With the same number of parameters (i.e., $|h_\psi| = m \times dim(\nu)$)[2] , IKL-NN outperforms IKL-RFF of $m = 128$ on Inception scores (6.876 versus 6.801). For IKL-RFF to achieve the same or better Inception scores of IKL-NN, the number of random features m needs increasing to 4096, which is less memory efficient than the IKL-NN realization. In particular, h_ψ of IKL-NN is a three-layers MLP with 2048 number of parameters ($16 \times 32 + 32 \times 32 + 32 \times 16$), while IKL-RFF has $2048, 65536$ number of parameters, for $m = 128, 4096$, respectively.

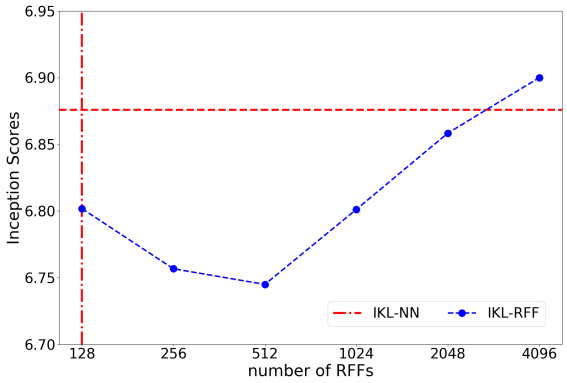

Figure 6: The comparison between IKL-NN and IKL-RFF on CIFAR-10 under different number of random features.

Algorithm	JS-4
IKL-NN	0.372 ± 0.002
IKL-RFF	0.383 ± 0.002
IKL-RFF (+2)	0.380 ± 0.002
IKL-RFF (+4)	0.377 ± 0.002
IKL-RFF (+8)	0.375 ± 0.002

Table 3: The comparison between IKL-NN and IKL-RFF on Google Billion Word.

On the other hand, using large m for IKL-RFF not only increases the number of parameters, but might also enhance the optimization difficulty. Zhang et al. (2017) discuss the difficulty of optimizing RFF directly on different tasks. Here we compare IKL-NN and IKL-RFF on challenging Google Billion Word dataset. We train IKL-RFF with the same setting as Section 3.3 and Appendix F.1, where we set the pool size m to be 1024 and the updating schedule between critic and generator to be $10 : 1$, but we tune the Adam optimization parameter for IKL-RFF for fair comparison. As discussed above, please note that the number of parameters for h_ψ is 2048 while IKL-RFF uses 16384 when $m = 1024$. The results are shown in Table 3. Even IKL-RFF is using more parameters, the performance 0.383 is not competitive as IKL-NN, which achieves 0.372.

In Algorithm 1, we update f_φ and h in each iteration with n_c times, where we use $n_c = 10$ here. We keep the number of updating f_φ to be 10, but increase the number of update for $\{\hat{\omega}_i\}_{i=1}^1 024$ to be $12, 14, 18$ in each iteration. The result is shown in Table 3 with symbols $+2$, $+4$ and $+8$ respectively. Clearly, we see IKL-RFF need

[2] $|h_\psi|$ denotes number of parameters in h_ψ, m is number of random features and $dim(\nu)$ is the dimension of the ν.

more number of updates to achieve competitive performance with IKL-NN. The results might implies IKL-RFF is a more difficult optimization problem with more parameters than IKL-NN. It also confirms the effectiveness of learning implicit generative models with deep neural networks Goodfellow et al. (2014), but the underlying theory is still an open research question. A better optimization algorithm Zhang et al. (2017) may improve the performance gap between IKL-NN and IKL-RFF, which worth more study as future work.

D Proof of Theorem 5

We first prove two Lemmas.

Lemma 7. *(Consistency with respect to data) With probability at least $1-\delta$, we have*

$$\sup_{h\in\mathcal{H}} |\hat{T}(k_h) - T(k_h)| \leq 2\mathbb{E}_X\left[\mathfrak{R}_X^{n-1}(\mathcal{F}_\mathcal{H})\right] + \sqrt{\frac{2}{n}\log\frac{1}{\delta}}$$

Proof. Define

$$\rho(x_1,\ldots,x_n) = \sup_{h\in\mathcal{H}} |\hat{T}(k_h) - T(k_h)|,$$

since $|k_h(x,x')| \leq 1$, it is clearly

$$\sup_{x_1,\ldots,x_i,x_i',\ldots,x_n} \quad |\rho(x_1,\ldots,x_i,\ldots x_n) - \rho(x_1,\ldots,x_i',\ldots x_n)| \leq \tfrac{2}{n}.$$

Applying McDiarmids Inequality, we get

$$\mathbb{P}\left(\rho(x_1,\ldots,x_n) - \mathbb{E}[\rho(x_1,\ldots,x_n)] \geq \epsilon\right) \leq \exp\left(\frac{-n\epsilon^2}{2}\right).$$

By Lemma 8, we can bound

$$\mathbb{E}[\rho(x_1,\ldots,x_n)] \leq 2\mathbb{E}_X\left[\mathfrak{R}_X^{n-1}(\mathcal{F}_\mathcal{H})\right]$$

and finish the proof. □

Lemma 8. *Given $X = \{x_1,\ldots,x_n\}$, define*

$$\rho(x_1,\ldots,x_n) = \sup_{h\in\mathcal{H}} |\hat{T}(k_h) - T(k_h)|,$$

we have

$$\mathbb{E}\Big[\rho(x_1,\ldots,x_n)\Big] \leq 2\mathbb{E}_X\left[\mathfrak{R}_X^{n-1}(\mathcal{F}_\mathcal{H})\right],$$

Proof. The proof is closely followed by Dziugaite et al. (2015). Given h, we first define $t_h(x,x') = s(x,x')k_h(x,x')$ as a new kernel function to simplify the notations. We are then able to write

$$\begin{aligned}
&\mathbb{E}\Big[\rho(x_1,\ldots,x_n)\Big] \\
=\ &\mathbb{E}_X\left[\sup_{h\in\mathcal{H}}\left|\mathbb{E}\Big[t_h(z,z')\Big] - \frac{1}{n(n-1)}\sum_{i\neq j} t_h(x_i,x_j)\right|\right] \\
\leq\ &\mathbb{E}_{X,Z}\left[\sup_{h\in\mathcal{H}}\left|\frac{1}{n(n-1)}\sum_{i\neq j}\left(t_h(z_i,z_j) - t_h(x_i,x_j)\right)\right|\right]
\end{aligned}$$

by using Jensen's inequality. Utilizing the conditional expectation and introducing the Rademacher random variables $\{\sigma_i\}_{i=1}^{n-1}$, we can write the above bound to be

$$\begin{aligned}&\frac{1}{n}\sum_i \mathbb{E}_{X_{-i},Z_{-i}}\mathbb{E}_{x_i,z_i}\left[\sup_{h\in\mathcal{H}}\left|\frac{\sum_{i\neq j} t_h(z_i,z_j)-t_h(x_i,x_j)}{n-1}\right|\right]\\ =\ &\mathbb{E}_{X,Z}\mathbb{E}_{X',Z',\sigma}\left[\sup_{h\in\mathcal{H}}\left|\frac{1}{n-1}\sum_{i=1}^{n-1}\sigma_i(t_h(z',z_n)-t_h(x',x_n))\right|\right] \qquad (11)\end{aligned}$$

The equality follows by $X-X'$ and $-(X-X')$ has the same distributions if X and X' are independent samples from the same distribution. Last, we can bound it by

$$\begin{aligned}&\leq \mathbb{E}_X\mathbb{E}_{\sigma,X'}\left[\sup_{h\in\mathcal{H}}\left|\frac{2}{n-1}\sum_{i=1}^{n-1}\sigma_i t_h(x',x_i)\right|\right]\\ &\leq \mathbb{E}_X\mathbb{E}_{\sigma}\left[\sup_{f\in\mathcal{F}_{k_\mathcal{H}}}\left|\frac{2}{n-1}\sum_{i=1}^{n-1}\sigma_i f(x_i)\right|\right]\\ &= 2\mathbb{E}_X[\mathfrak{R}_X^{n-1}(\mathcal{F}_\mathcal{H})]\end{aligned}$$

The second inequality follows by $s(x,x')\phi(x')\in\mathcal{F}$ since $|s(x,x')|\leq 1$.

□

Lemma 9. *(Consistency with respect to sampling random features) With probability $1-\delta$, we have*

$$|\sup_{h\in\mathcal{H}}\hat{T}(k_h)-\sup_{h\in\mathcal{H}}\hat{T}(\hat{k}_h)|\leq\sqrt{\frac{2\log\frac{4}{\delta}}{m}}$$

Proof. Let the optimal solutions be

$$\begin{aligned}h^* &= \arg\max_{h\in\mathcal{H}}\hat{T}(k_h)\\ \hat{h} &= \arg\max_{h\in\mathcal{H}}\hat{T}(\hat{k}_h),\end{aligned}$$

By definition,

$$\begin{aligned}&\hat{T}(\hat{k}_h)\\ =\ &\frac{1}{n(n-1)}\sum_{i\neq j}s_{ij}\left(\frac{1}{m}\sum_{k=1}^{m}\cos(h(\nu_k)^\top(x_i-x_j))\right)\\ =\ &\frac{1}{m}\sum_{k=1}^{m}\left(\frac{1}{n(n-1)}s_{ij}\cos(h(\nu_k)^\top(x_i-x_j))\right)\end{aligned}$$

It is true that $|\frac{1}{n(n-1)}s_{ij}\cos(h(\nu_k)^\top(x_i-x_j)|\leq 1$ since $|s_{ij}|<1$ and $|\cos(x)|<1$. we then have

$$\begin{aligned}&\mathbb{P}(|\sup_{h\in\mathcal{H}}\hat{T}(k_h)-\sup_{h\in\mathcal{H}}\hat{T}(\hat{k}_h)|>\epsilon)\\ \leq\ &\mathbb{P}(|\hat{T}(k_{h^*})-\hat{T}(\hat{k}_{h^*})|>\epsilon)+\mathbb{P}(|\hat{T}(k_{\hat{h}})-\hat{T}(\hat{k}_{\hat{h}})|>\epsilon)\\ \leq\ &4\exp\left(-\frac{m\epsilon^2}{2}\right),\end{aligned}$$

where the last inequality follows from the Hoeffding's inequality. □

With Lemma 7 and Lemma 9, we are ready to prove Theorem 5. We can decompose

$$\begin{aligned}&|T(\hat{k}_{\hat{h}})-\sup_{h\in\mathcal{H}}T(k_h)|\\ \leq\ &|\sup_{h\in\mathcal{H}}T(k_h)-\sup_{h\in\mathcal{H}}\hat{T}(k_h)|+|\sup_{h\in\mathcal{H}}\hat{T}(k_h)-\hat{T}(\hat{k}_{\hat{h}})|+|\hat{T}(\hat{k}_{\hat{h}})-T(\hat{k}_{\hat{h}})|\\ \leq\ &\sup_{h\in\mathcal{H}}|T(k_h)-\hat{T}(k_h)|+|\sup_{h\in\mathcal{H}}\hat{T}(k_h)-\hat{T}(\hat{k}_{\hat{h}})|+\sup_{h\in\mathcal{H}}|\hat{T}(\hat{k}_h)-T(\hat{k}_h)|\end{aligned}$$

We then bound the first and third terms by Lemma 7 and the second term by Lemma 9. Last, using a union bound completes the proof.

E Generalization of Random Kitchen Sinks with IKL

Theorem 10. *(Generalization (Cortes et al., 2010)) Define the true and empirical misclassification for a classifier* f *as* $R(f) = \mathbb{P}(Yf(X) < 0)$ *and* $\hat{R}_\gamma(h) = \frac{1}{n}\sum_{i=1}^n \min\{1, [1 - yf(x_i)/\gamma]_+\}$. *Then*

$$\sup_{f \in \hat{\mathcal{F}}_{\mathcal{H}}} \{R(f) - \hat{R}_\gamma(f)\} \leq \frac{2}{\gamma}\mathfrak{R}_X^n(\hat{\mathcal{F}}_{\mathcal{H}}) + 3\sqrt{\frac{\log\frac{2}{\delta}}{2n}}$$

with probability at least $1 - \delta$.

F Hyperparameters

We report the hyperparameters used in the experiments.

F.1 GAN

For Gaussian kernels, we use $\sigma_q = \{1, 2, 4, 8, 16\}$ for images and $\sigma_q = \{0.5, 1, 2, 4, 8\}$ for text; for RQ kernels, we use $\alpha_q = \{0.2, 0.5, 1, 2, 5\}$ for images and $\alpha_q = \{0.04, 0.1, 0.2, 0.4, 1\}$ for text. We used Adam as optimizer. The learning rate for training both f_ϕ and g_θ is 0.0005 and 0.0001 for image and text experiments, respectively. The batch size B is 64. We set hyperparameter n_c for updating critic to be $n_c = 5$ and $n_c = 10$ for CIFAR10 and Google Billion Word datasets. The learning rate of of h_ψ for Adam is 10^{-6}.

F.2 Random Kitchen Sinks with IKL

For OPT-KL, we use the code provided by Sinha and Duchi (2016)[3]. We tune the hyperparameter $\rho = \{1.25, 1.5, 2, 4, 16, 64\}$ on the validation set. For RFF, OPT-KL, and IKL, the linear classifier is Logistic Regression Fan et al. (2008)[4], as to make reasonable comparison with MLP. We use 3-fold cross validation to select the best C on training set and present the error rate on test set. For CIFAR-10 and MNIST, we normalize data to be zero mean and one standard deviation in each feature dimension. The learning rate for Adam is 10^{-6}. We follow Bullins et al. (2018) to use early stopping when performance on validation set does not gain.

[3] https://github.com/amansinha/learning-kernels
[4] https://github.com/cjlin1/liblinear